JVSTB
Journal of Vacuum Science & Technology B

High resolution nanofabrication using self-assembly of metal salt-polymer nanocomposite film

Celal Con, Ferhat Aydinoglu, and Bo Cui

Citation: Journal of Vacuum Science & Technology B **33**, 06F304 (2015); doi: 10.1116/1.4935654
View online: http://dx.doi.org/10.1116/1.4935654
View Table of Contents: http://scitation.aip.org/content/avs/journal/jvstb/33/6?ver=pdfcov
Published by the AVS: Science & Technology of Materials, Interfaces, and Processing

Articles you may be interested in

Hierarchical self-assembly of nanoparticles in polymer matrix and the nature of the interparticle interaction
J. Chem. Phys. **142**, 214905 (2015); 10.1063/1.4921567

Synergistic effect of self-assembled carboxylic acid-functionalized carbon nanotubes and carbon fiber for improved electro-activated polymeric shape-memory nanocomposite
Appl. Phys. Lett. **102**, 231910 (2013); 10.1063/1.4811134

Why specific mixed solvent composition leads to appropriate film formation of composite during spin coating?
Appl. Phys. Lett. **102**, 051918 (2013); 10.1063/1.4791696

Diblock copolymer based self-assembled nanomagnetoelectric
Appl. Phys. Lett. **93**, 173507 (2008); 10.1063/1.3005558

Self-assembled ordered polymer nanocomposites directed by attractive particles
J. Chem. Phys. **128**, 164903 (2008); 10.1063/1.2907744

HIDEN ANALYTICAL
Instruments for Advanced Science

Gas Analysis
- dynamic measurement of reaction gas streams
- catalysis and thermal analysis
- molecular beam studies
- dissolved species probes
- fermentation, environmental and ecological studies

Surface Science
- UHV TPD
- SIMS
- end point detection in ion beam etch
- elemental imaging - surface mapping

Plasma Diagnostics
- plasma source characterization etch and deposition process reaction
- kinetic studies
- analysis of neutral and radical species

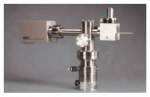
Vacuum Analysis
- partial pressure measurement and control of process gases
- reactive sputter process control
- vacuum diagnostics
- vacuum coating process monitoring

Contact Hiden Analytical for further details:
W www.HidenAnalytical.com
E info@hiden.co.uk
CLICK TO VIEW our product catalogue

Redistribution subject to AVS license or copyright; see http://scitation.aip.org/termsconditions. Download to IP: 129.97.40.81 On: Wed, 18 Nov 2015 22:45:48

High resolution nanofabrication using self-assembly of metal salt-polymer nanocomposite film

Celal Con,[a] Ferhat Aydinoglu, and Bo Cui
Waterloo Institute for Nanotechnology (WIN), University of Waterloo, 200 University Ave. West, Waterloo, Ontario N2L 3G1, Canada

(Received 3 August 2015; accepted 2 November 2015; published 12 November 2015)

For fabrication of nanostructures that do not need long range ordering and precise placement, such as antireflective structure for photovoltaic and display applications and super-hydrophobic surface for lab-on-chip applications, bottom-up fabrication techniques are more preferable than top-down techniques due to their low cost. Here, the authors report a simple process to obtain nanostructures using low-cost spin-coating method and pattern transfer. They first dissolved metal salt and polymer in a solvent. After spin-coating to form a thin film, the authors annealed the film to attain a phase separation. Next, the nanocomposite film was etched with oxygen plasma to remove the polymer matrix, leaving behind nanoscale metal salt islands that can be used as a hard mask for dry etching the substrate or sublayer. With optimal metal salt (nickel nitrate hexahydrate) and polymer (polymethylmethacrylate) weight ratio, the authors achieved wafer-scale high resolution (down to 20 nm) pillar structures etched in silicon with 100 nm height and ~100 nm spacing. © *2015 American Vacuum Society*. [http://dx.doi.org/10.1116/1.4935654]

I. INTRODUCTION AND MOTIVATION

Surface nanostructures without long range ordering and precise placement have a wide range of applications. For instance, they can be used as antireflective coating for photovoltaic devices where the reflection of incident light from the substrate surface is greatly reduced to improve their efficiency. In flat panel display or imaging applications, they can be employed to increase transmission and eliminate ghost image or veil glare.[1] These nanostructures can also mimic and follow the nature's example such as lotus leaves to make super-hydrophobic surfaces, or gecko feet for adhesive surfaces.[1–4]

These nanostructures can be fabricated via top-down lithography techniques—including photolithography, electron-beam lithography, and nanoimprint lithography—and bottom-up lithography approaches that are commonly called self-assembly lithography. The top-down lithography techniques, while offering more precise control of the shape, size, and placement of the nanostructures, usually require sophisticated and expensive equipment. Among them, nanoimprint lithography is the most promising one since it is relatively a low-cost and high throughput process with ultrahigh resolution capability, though the mold has to be fabricated by other costly lithography. On the other hand, self-assembly lithography is undoubtedly much cheaper than top-down lithography techniques, though it can only achieve either random or periodic patterns without long range ordering unless otherwise guided. The most popular self-assembly lithography is the so-called nanosphere lithography where nanosized spheres are assembled to form periodic structures. Yet it is challenging to form uniform monolayer sphere for sub-100 nm sphere size.[5] In recent years, self-assembly of diblock copolymer is gaining increasing popularity, but the process can be lengthy and very sensitive to substrate preparation, and feature size over 100 nm is hard to obtain. Another technique to create surface nanostructures makes use of the self-masking effect in reactive ion etching that leads to the formation of "grass"[6] structure notably "black silicon."[7] Besides silicon, polymer can also be nanotextured by plasma etching.[8–10] This roughness instability is due to deposition coming from sputtering of irremovable materials from the metallic or dielectric reactor wall, which acts as hard mask during the polymer etching. Moreover, under certain optimal conditions, ordered periodic morphology can be induced on plasma-etched polymeric surfaces.[10]

The next self-assembly technique is the deposition of metal film on a substrate followed by thermal annealing to achieve submicrometer sized metal islands that can be used as hard mask for etching the substrate.[11–13] Lastly, CsCl film can be thermally evaporated to form nanoislands as etching mask upon exposure to humidity after film deposition.[14] However, these techniques based on island film both need high cost vacuum deposition tool.

Here, we report a simple process to obtain nanostructures using low-cost spin-coating method and RIE pattern transfer. We dissolved metal salt and polymer in a solvent; and after forming a thin film by spin-coating and thermal annealing to attain a phase separation, the nanocomposite film was etched with oxygen plasma to remove the polymer matrix, leaving behind nanoscale metal salt islands on the substrate that can be used as a hard-mask to dry-etch the substrate or sublayer (shown in Fig. 1). We show that with our method, it is possible to achieve sub-20 nm resolution nanostructures on the substrate surface, though it does not give a periodic structure.

II. EXPERIMENTAL METHODS

For our purpose, we have investigated several metal salts containing nickel metal. Nickel is a very hard etching mask

[a]Electronic mail: ccon@uwaterloo.ca

Redistribution subject to AVS license or copyright; see http://scitation.aip.org/termsconditions. Download to IP: 129.97.40.81 On: Wed, 18 Nov 2015 22:45:48

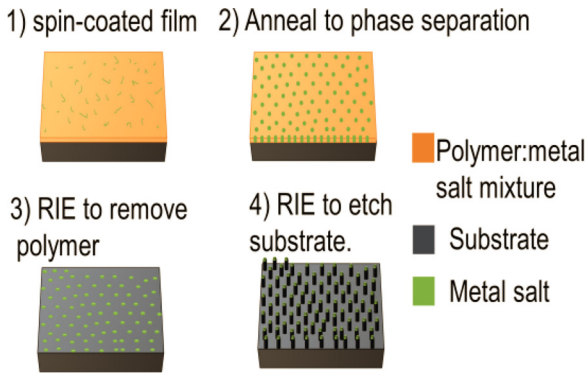

FIG. 1. (Color online) Fabrication process of ultrahigh resolution nanostructures using self-assembly of metal salt-polymer nanocomposite film. (1) Spin-coating film from a solution containing polymer and salt. (2) Phase separation by thermal annealing. (3) Etching polymer using oxygen plasma and leaving behind metal salt nanoislands on silicon. (4) Etching silicon using fluorine based plasma (CF_4 gases) with metal salt nanoislands as mask.

for reactive ion etching using both fluorine and chlorine based plasmas that can create surface nanostructures. Nickel is found in the form of nickel (II) sulfate, nickel (II) nitrate, and nickel (II) chloride hexahydrate. Recently, nickel chloride hexahydrate is reported as a metal salt miscible with polymer (polymethylmethacrylate) (PMMA) resist to increase its etching resistance by four times.[15] Unlike salt-containing electron beam resist for lithography, for the purpose of creating nanostructures by self-assembly, the mixture needs to phase-separate. As nickel (II) nitrate hexahydrate [$Ni(NO_3)_2{\cdot}6H_2O$] has a low melting temperature (56.7 °C), phase-separation can be attained readily by thermal annealing.

In the experiment, we first dissolved PMMA powder (996 kg/mol, Sigma Aldrich) with 10 wt./vol. % concentration in dimethylformamide (DMF). In parallel, we dissolved nickel nitrate hexahydrate (99.999% purity, Sigma Aldrich) in DMF with varying concentrations of 1–10 wt./vol. %. Afterwards, we mixed the as-prepared PMMA solution and salt solution with 1:1 volume ratio and obtained a uniform clear solution. As such, the final solution for spin-coating contains 0.5–5 wt./vol. % nickel salt and 5 wt./vol. % PMMA, leading to a weight ratio of nickel salt and PMMA ranging from 1:10 to 10:10.

The fabrication process for nanostructured silicon as an example is shown in Fig. 1. We cleaned the silicon substrate by solvent and oxygen plasma, and coated 100 nm PMMA on silicon. This layer of pure PMMA film was found to help attain a more uniform film of the PMMA-salt mixture. Then, the mixture was spin-coated on PMMA film, to obtain a 300 nm-thick film for the case with 10:1 weight ratio of PMMA:metal (obtained by mixing at equal volume 10 wt./vol. % PMMA solution and 1 wt./vol. % salt solution, both in DMF). Thermal annealing was carried out at 120 °C for 1 h to induce phase separation between polymer and the salt. To evaluate the potential intermixing with the bottom PMMA layer, we spin-coated PMMA dissolved in DMF on the bottom PMMA layer, and found the total film thickness was the sum of the top and bottom PMMA films. Hence, the bottom PMMA is not significantly dissolved by DMF during the spin-coating, and there should be negligible intermixing between the PMMA-salt composite and bottom PMMA layer. We also spin-coated a polystyrene film (glass transition temperature close to that of PMMA, low Flory–Huggins interaction parameter with PMMA and thus relatively easy interdiffusion) on the bottom PMMA layer and annealed the film stack at 120 °C for 5 min. After selectively dissolving the top polystyrene layer using xylene, the remaining PMMA film had a smooth surface, indicating negligible intermixing occurs during the thermal annealing. Therefore, we expect the intermixing between the PMMA-salt composite and bottom PMMA layer is negligible.

Next, we conducted oxygen plasma etching using Trion Phantom II ICP-RIE system (20 sccm O_2, 20 W RF power, 0 W ICP power, 100 mTorr, room temperature, and etches PMMA 100 nm/min) to remove PMMA without significant attack of metal salt, leaving behind nickel nitrate nanoislands on silicon as seen in Fig. 2. As a final step, we etched silicon by RIE using CF_4 gas (20 sccm CF_4, 100 W RF power, 0 W ICP power, 20 mTorr, room temperature; etching rates for silicon, PMMA, and metal salt are 30, 300, and roughly 10 nm/min, respectively) with the salt nanoislands as hard etching mask.

III. RESULTS AND DISCUSSION

The main challenge is to find a solvent that can dissolve both PMMA and metal salt, because salts are typically soluble in water whereas polymers are commonly soluble in organic solvents. Broadly speaking, solvents are categorized as nonpolar solvent such as benzene and toluene, polar aprotic solvent such as tetrahydrofuran (THF), acetone, and DMF, and polar protic solvent such as ethanol, acetic acid, and water. After extensive search and trial, we found that this nickel salt is soluble in solvents including THF, DMF, and acetic acid, all of which can also dissolve PMMA. Atomic force microscopy (dimension 3100, tapping mode using standard silicon tip) images are shown in Fig. 3. Only DMF gave a uniform and smooth film with a rms value of 5.0 nm after spin-coating and thermal annealing, and the other two solvents gave very rough films with a rms value of 26.1 and 27.1 nm for acetic and THF, respectively. Hence, we chose DMF solvent, which is a polar aprotic solvent having a boiling temperature of 153 °C. As for the polymer, we studied only PMMA that is a well-known electron-beam lithography resist and is very popular with low cost.

After PMMA removal by oxygen plasma etching and pattern transfer into silicon using CF_4 gas RIE, the obtained self-assembled nanostructures are shown in Fig. 4, by using Zeiss UltraPlus FESEM. We obtained dense, with the diameters average to be 40.5 nm [Figs. 4(a) and 4(b)] and a standard deviation of 12.46 nm pillars with 100 nm height by using nickel nitrate and PMMA nanocomposite with mass ratio of 1:10 (i.e., the weight concentration for PMMA in the DMF solution is ten times that of the nickel nitrate hexahydrate), and the pillar diameters are relatively uniform, though

Redistribution subject to AVS license or copyright; see http://scitation.aip.org/termsconditions. Download to IP: 129.97.40.81 On: Wed, 18 Nov 2015 22:45:48

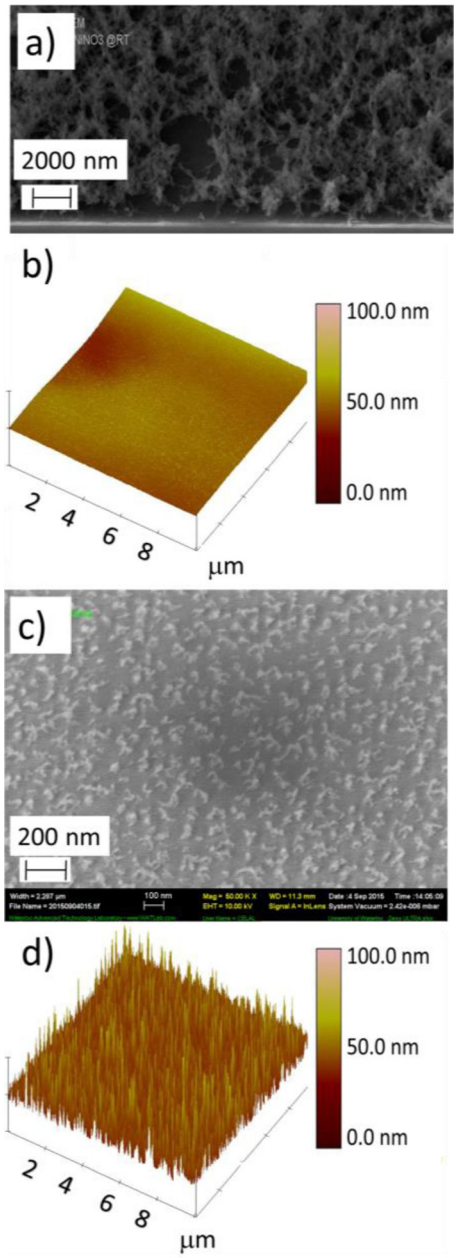

FIG. 2. (Color online) (a) SEM image of the thin film of PMMA:nickel (II) nitrate hexahydrate 10:1 wt. % after spin-coated, without immediate baking, nonuniform film formation is observed. (b) AFM image of the same film after annealing at 120 °C, which introduced uniform film distribution and phase separation. (c) SEM image of the film upon oxygen plasma removed all polymer film and left behind nanosized metal salt islands. (d) AFM image of the film upon oxygen plasma removed all polymer film and left behind nanosized metal salt islands.

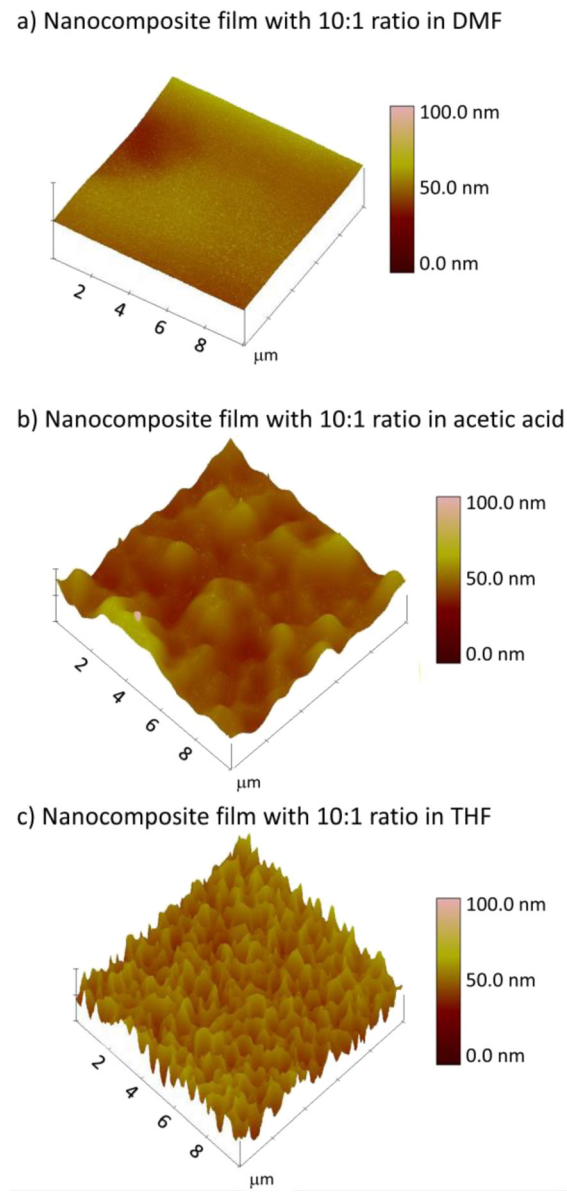

FIG. 3. (Color online) AFM images of the thin film of PMMA:nickel (II) nitrate hexahydrate, dissolved for spin-coating in (a) DMF, (b) acetic acid, and (c) THF, respectively. Nanocomposite film inside DMF gives less roughness (5.0 nm) than others (26.1 nm with acetic acid and 27.1 nm with THF).

the pillar location is rather random without short or long range ordering.

For this weight ratio, it can be calculated that on average each methylmetharcylate (MMA) monomer contains 0.034 Ni atom (alternatively, 1 nickel atom in every 29.0 MMA monomers). As we increased the amount of nickel salt inside PMMA to a ratio of 2:10–5:10 [Figs. 4(c)–4(e)], pillars became larger that is expected, and the structure became less well defined. Further increase of the salt in PMMA to a ratio of 7:10 and 10:10 resulted in poorly defined nanostructure [Figs. 4(f)–4(g)], implying that salt islands were agglomerated to form quasicontinuous film.

As the salt consists of a large amount of hydrate (here hexahydrate), it might be decomposed (dehydrated) during the thermal annealing process. Thermal decomposition of metal salts including nickel nitrate has been well studied[16–21] under atmospheric or nitrogen environment by monitoring the reactions occurring throughout the decomposition up to 600 °C by means of thermogravimetry analysis (TGA) and differential thermal analysis (DTA).[19] These works reported that, with thermal treatment at low pressures ($\leq$5 mbar), only decomposition/dehydration products (tetrahydrate, dihydrate, and anhydrous nickel nitrate) are obtained in the first step.[22] Additional study at high temperatures of above

Redistribution subject to AVS license or copyright; see http://scitation.aip.org/termsconditions. Download to IP: 129.97.40.81 On: Wed, 18 Nov 2015 22:45:48

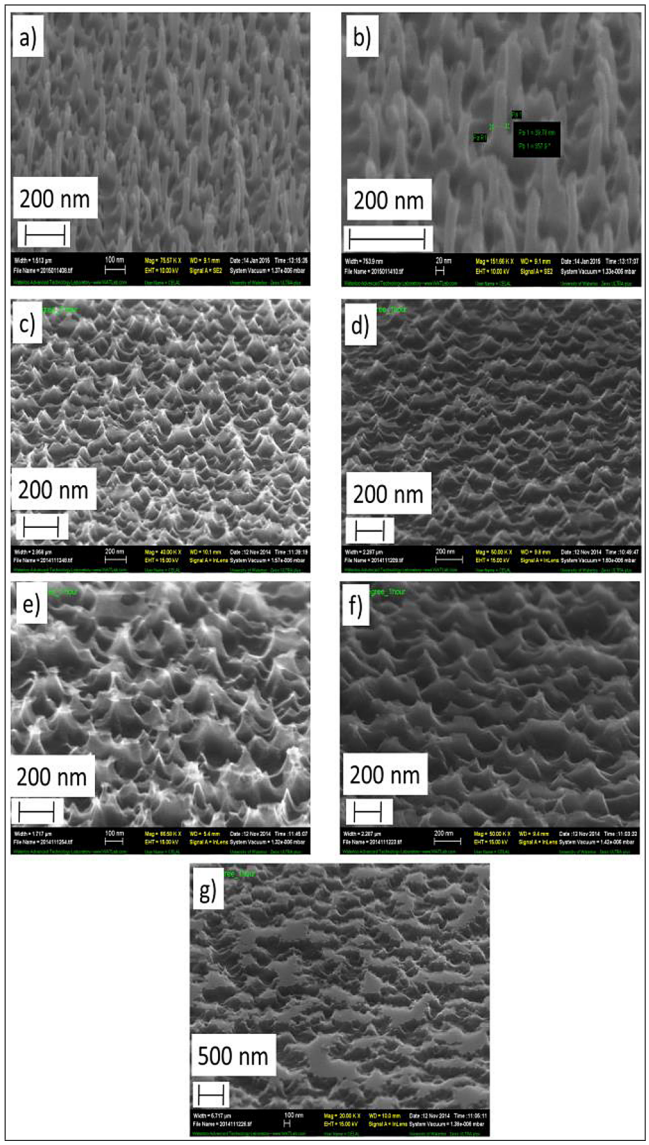

FIG. 4. (Color online) SEM images of silicon nanostructures, etched using phase-separated nickel (II) nitrate metal salt:PMMA film as a mask with different weight ratio. (a) and (b) 1:10, (c) 2:10, (d) 3:10, (e) 5:10, (f) 7:10, and (g) 10:10. It is observed that with 10:1 ratio film, some pillars with diameter less than 20 nm are formed.

200 °C and low pressure conditions suggests the presence of intermediate compounds with different characteristics, which eventually give place to NiO with different surface properties.[22] Under atmospheric conditions, Elmasry *et al.*[21] reported that decomposition/dehydration starts at low temperatures by losing water, and the nickel salt becomes anhydrous ($Ni(NO_3)_2$) at 205 °C, where 37% mass is lost and constant mass is maintained above 205 °C till 303 °C, where the salt turns into $Ni_2(OH)_2$ and becomes nickel oxide (NiO) at 505 °C along with a mass loss of 73.3% of its original mass.

According to the TGA by Elmasry *et al.*,[21] our annealing at 120 °C at atmospheric condition would lead to a ~12% mass loss, corresponding to a drop in molecular weight from 290.79 to 255.89 g/mol by forming $Ni(NO_3)_2{\cdot}4.1H_2O$.

Lastly, similar hard mask for etching the substrate can also be obtained by mixing metal or metal compound nanoparticle with a polymer, followed by etching away the polymer using oxygen plasma. Nanocomposite consisting of metal nanoparticle dispersed in a polymer matrix is considered as a single homogeneous material with unique thermal, mechanical, and biological properties when compared to conventional composite.[23,24] Yet, it is challenging to disperse evenly the nanoparticle into a polymer matrix, and typically, the nanoparticle surface has to be functionalized to avoid agglomeration and attain even distribution in the solvent for spin-coating to form a film. Our method is advantageous in that the final feature size can be tuned by adjusting the salt-polymer weight ratio or annealing conditions, whereas the nanoparticle composite gives only a fixed feature size equal to the particle diameter.

IV. CONCLUSION

We developed a simple process to obtain nanostructures using the low-cost spin-coating method and RIE pattern transfer. We dissolved metal salt and polymer in a solvent; and after spin-coating to form a thin film and thermal annealing to attain a phase separation, the nanocomposite was etched with oxygen plasma to remove the polymer matrix, leaving behind nanoscale salt islands on the substrate that can be used as a hard-mask to dry-etch the substrate or sublayer. The key challenge for our process is to identify a solvent or solvent mixture that can dissolve both the salt (commonly soluble in water) and polymer (commonly soluble only in organic solvent). After extensive testing, we found that nickel (II) nitrate hexahydrate and PMMA can be dissolved in DMF and form a uniform film by spin-coating. Nickel nitrate is a suitable salt since nickel is a very hard mask for RIE using both F- and Cl-plasmas, and it has a low melting temperature of 56.7 °C. It is calculated that 10:1 weight ratio of PMMA and salt corresponds to 1 nickel atom in every 29.0 MMA monomers. Using this method with optimum weight ratio of 1:10, we are able to achieve a very high resolution (down to 20 nm) silicon nanopillars with 100 nm height and ~100 nm spacing at low cost and wafer-scale high throughput.

ACKNOWLEDGMENTS

This work was carried out using the nanofabrication facility at Giga-to-Nanoelectronics Laboratory funded by the Canada Foundation for Innovation, the Ontario Ministry of Research and Innovation, and Industry Canada. C.C. and F.A. acknowledge The Ministry of Turkish National Education for financially supporting their study.

[1]D. Kontziampasis, G. Boulousis, A. Smymakis, K. Ellinas, A. Tserepi, and E. Gogolides, Microelectron. Eng. **121**, 33 (2014).
[2]E. Stratakis, A. Ranella, and C. Fotakis, Biomicrofluidics **5**, 013411 (2011).
[3]T. Taguchi, H. Hayashi, A. Fujii, K. Tsuda, N. Yamada, K. Mineura, A. Isurugi, I. Ihara, and Y. Itoh, SID Symp. Dig. Tech. Pap. **41**, 1196 (2010).
[4]S. Tawfick, M. De Volder, D. Copic, S. Park, C. R. Oliver, E. S. Polsen, M. J. Roberts, and A. J. Hart, Adv. Mater. **24**, 1628 (2012).
[5]J. C. Hulteen and R. P. Van Duyne, J. Vac. Sci. Technol., A **13**, 1553 (1995).

Redistribution subject to AVS license or copyright; see http://scitation.aip.org/termsconditions. Download to IP: 129.97.40.81 On: Wed, 18 Nov 2015 22:45:48

[6]M. Gharghi and S. Sivoththaman, J. Vac. Sci. Technol., A **24**, 723 (2006).
[7]H. V. Jansen, M. J. de Boer, S. Unnikrishnan, M. C. Louwerse, and M. C. Elwenspoek, J. Micromech. Microeng. **19**, 033001 (2009).
[8]E. Gogolides, V. Constantoudis, G. Kokkoris, D. Kontziampasis, K. Tsougeni, G. Boulousis, M. Vlachopoulou, and A. Tserepi, J. Phys. D: Appl. Phys. **44**, 174021 (2011).
[9]D. Kontziampasis, V. Constantoudis, and E. Gogolides, Plasma Processes Polym. **9**, 866 (2012).
[10]N. Vourdas, D. Kontziampasis, G. Kokkoris, V. Constantoudis, A. Goodyear, A. Tserepi, M. Cooke, and E. Gogolides, Nanotechnology **21**, 085302 (2010).
[11]S. Wang, X. Z. Yu, and H. T. Fan, Appl. Phys. Lett. **91**, 061105 (2007).
[12]G. Lin, Y. Chang, E. Liu, H. Kuo, and H. Lin, Appl. Phys. Lett. **90**, 181923 (2007).
[13]J. W. Leem, K. S. Chung, and J. S. Yu, Curr. Appl. Phys. **12**, 291 (2012).
[14]W. Liu, M. Ferguson, M. Yavuz, and B. Cui, J. Vac. Sci. Technol., B **30**, 06F201 (2012).
[15]C. Con and B. Cui, paper presented at the 59th EIPBN, San Diego, CA (2015).
[16]P. Thomasson, O. S. Tyagib, and H. Knozinger, Appl. Catal. A Gen. **181**, 181 (1999).
[17]E. Ruckenstein and Y. H. Hu, Appl. Catal. A Gen. **183**, 85 (1999).
[18]B. Jankovic, S. Mentus, and D. Jelic, Physica B **404**, 2263 (2009).
[19]W. Brockner, C. Ehrhardt, and M. Gjikaj, Thermochim. Acta **456**, 64 (2007).
[20]A. M. Gadalla and H. Yu, J. Thermal Anal. **37**, 319 (1991).
[21]M. A. A. Elmasry, A. Gaber, and E. M. H. Khater, J. Thermal Anal. **52**, 489 (1998).
[22]J. Estelle, P. Salagre, Y. Cesteros, M. Serra, F. Medina, and J. E. Sueiras, Solid State Ionics **156**, 233 (2003).
[23]A. C. Balazs, T. Emrick, and T. P. Russell, Science **314**, 1107 (2006).
[24]E. Tang, G. Cheng, and X. Ma, Powder Technol. **161**, 209 (2006).

Redistribution subject to AVS license or copyright; see http://scitation.aip.org/termsconditions. Download to IP: 129.97.40.81 On: Wed, 18 Nov 2015 22:45:48